euspen's 21st International Conference & Exhibition, Copenhagen, DK, June 2021
www.euspen.eu

Precision manufacture of concrete parts using Integrated Robotic 3D Printing and Milling

Peter Kinnell[1], James Dobranski[2], Jie Xu[2], Weiqiang Wang[2], John Kolawole[2], John Hodgson[1], Simon Austin[2], John Provis[3], Sergio Cavalaro[2], Richard Buswell[2]

[1] *Wolfson School of Mechanical Electrical and Manufacturing Engineering, Loughborough University, Loughborough, UK.*
[2] *School of Architecture, Building and Civil Engineering, Loughborough University, Loughborough, UK.*
[3] *Department of Materials Science and Engineering, The University of Sheffield, Sheffield, UK.*

P.Kinnell@lboro.ac.uk

Abstract

When manufacturing free-form concrete parts, casting approaches are most commonly adopted. While casting allows good surface finish, geometric repeatability and easy replication of parts, it is inflexible and costly to setup. Expensive mould tools, with limited life, must be created before manufacturing can begin. These mould tools must then be safely stored to ensure future identical parts can be manufactured. If damaged, recreating exact replica mould tooling is an expensive and time-consuming process. The cost and difficulty of manufacturing new tooling therefore prohibits the economic manufacture of many bespoke parts, or results in significant lead time increases and project delays. An alternative approach, that is gaining increasing interest, is the use of 3D printing for concrete. A robot is used to guide a concrete deposition nozzle in a layer by layer deposition path, similar to polymer fused deposition modelling. However, in Concrete 3D Printing the combination of complex material rheological properties, and the need for high volumetric deposition rates, means achieving net shape precision parts from the deposition step is extremely challenging. To address this issue, a hybrid robotic 3D printing and milling system has been developed, with integrated in-process structured-light metrology, to enable the production of precision concrete parts with well controlled geometric features. The integrated robot manufacturing cell is described. Examples structures that demonstrate the ability to create and replicate complex concrete parts with improved surface properties are illustrated. Components with surface features that enable concrete assemblies are studied to illustrate the capability of the hybrid process to manufacture challenging parts with demanding geometric requirements. These structures are used to quantify the performance of the current system and illustrate the future potential for the approach.

Manufacturing (CAM), 3D Printing, Milling, Robot

1. Introduction

3D concrete printing or 3DCP, has been in development for the past 15-20 years. The first 3DCP system developed as an off-site manufacturing process was developed from 2006-2008 at Loughborough University [1, 2, 3]. Since this work, the technology has achieved increasing attention from many academic institutions, research and technical organisations and industry. Applications for 3DCP range from large-scale robotic manufacturing of housing, where manufacturing speed and efficiency are the goal, to bespoke production of concrete parts for specialist construction applications, were flexibility, lead-time and eliminating costly special-purpose tooling are the key drivers [4 - 9].

Currently, Casting is the most common approach for manufacturing concrete parts. Casting has the benefit of being able to produce objects with good surface finish, repeatable dimensions, and allows for low-skill easy replication of many parts. This is ideal for mass produced objects, where the initial cost of setup, such as the production of mould tooling can be easily justified. However, mould tools have a limited life, and the repair and replacement of the tooling must be factored in to production costs. For complicated objects, with intricate features, mould tool manufacture is a difficult, expensive and a skilled task. Achieving precise replication, which can be important for aesthetic or functional reasons, can be a challenging process. The cost and difficulty of manufacturing mould tooling therefore prohibits the economic manufacture of many bespoke parts, that are required in low quantities, or adds significant cost and time to projects where the parts are absolutely required, such as for repair or restoration work.

2. Digital manufacturing for concrete parts

Digital manufacturing approaches can provide an alternative to traditional casting, by combining robotic 3DCP with a complementary subtractive process. A serial industrial robot is used to guide a concrete deposition nozzle in a layer-by-layer deposition path. Wet concrete is extruded from the nozzle to deposit a continuous filament of material, like polymer fused deposition modelling. However due to the non-ideal material rheological properties of the extruded concrete, and the economic need for high deposition rates, which calls for large diameter filaments, achieving true net-shape parts from the deposition step is extremely challenging. To give an idea of the typical level of precision necessary for concrete construction, tolerances of +/- 5 mm might be expected on the opening dimensions needed for fitting a typical window of a few meters in size [10]; +/- 0.3 to 1.6 mm could be specified on the width of

2 m wide concrete curved tunnel lining segments, or +/- 2 to 6.4 mm for the thickness of these segments that are nominally between 300 and 500 mm in thickness [11]. While tolerances of the order of a few millimetres are relatively large in the context of traditional precision engineering, they represent a reasonable challenge for 3D printing of concrete parts. To improve part precision, in this work a hybrid 3DCP and milling system has been developed, with integrated structured-light metrology, to enable the production of precision concrete parts with well controlled geometric features.

2.1. Hybrid 3DCP for material deposition and precision removal

An ABB IRB 6640 robot was used as the basis for the deposition and milling system. The robot was equipped with a tool mounting flange to allow easier change over from deposition to milling. In figure 1, the robot can be seen with the deposition nozzle attached. Premixed wet concrete is stored in a hopper adjacent to the robot. An m-tec P20V screw pump is used to pump premixed concrete through a hose to the deposition nozzle that is fixed to the robot tool mounting flange.

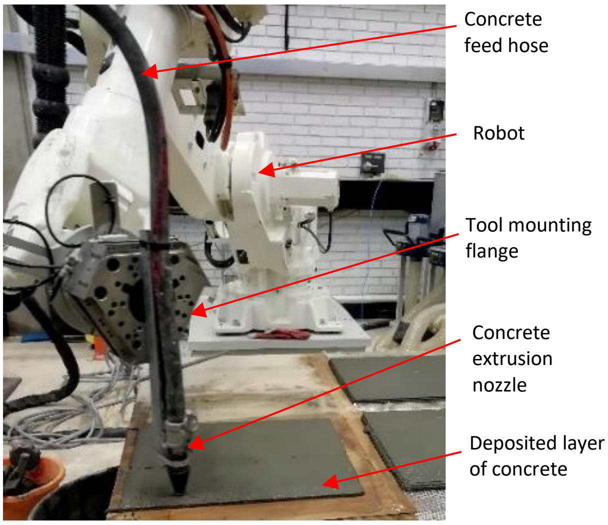

Figure 1. Photograph of the Hybrid 3DCP robot in deposition mode.

In figure 2 the robot can be seen with the milling tool in place. A spindle motor is attached to the tool mounting flange, with power and control cables connecting the spindle with the control unit. The milling tool used was a non-coated ball nose flute cutter, with a diameter of 16 mm and a spindle of 2000 rpm was used for milling.

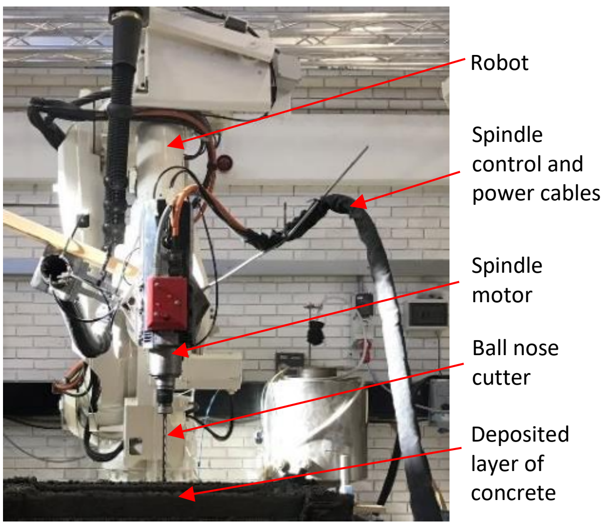

Figure 2. Photograph of the Hybrid 3DCP robot in milling mode.

2.2. Measurement system

A re-configurable fringe projection 3D scanner was custom built for use with the hybrid 3DCP system. HP Scan Pro v5 software was selected as this provides a simple calibration and scanning framework, and allows for the modular combination of user selected components. This allows for a high-performance scanning system to be created and configured for the exact scanning needs required. In this case, a CASIO XJ-F100W projector was selected for its relatively small aperture (f2.5) for a projector, high brightness of 3500 lm and illumination technology (Laser & LED). This gives good depth of focus and the LED and laser illumination is robust to vibration. For the cameras, two 12 mega-pixel Basler acA4096-30um were selected using 16 mm lenses. For the scanner baseline, a 50 mm diameter carbon fibre tube was selected to provide good torsional and bending stiffness, as well as low coefficient of thermal expansion.

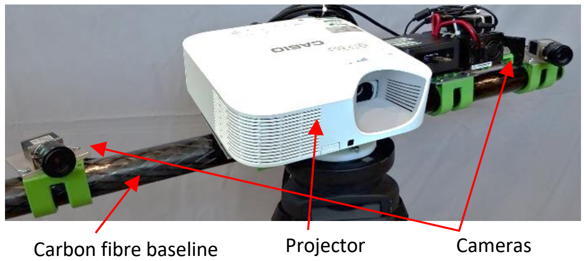

Figure 3. Custom built, reconfigurable structured light 3D scanner.

3. Scanner performance evaluation

A basic performance evaluation of the scanner was undertaken to access point noise and geometric measurement uncertainty. Point noise was measured using a plane artefact that was a machined flat, lightly sand-blasted, 20 mm thick 400 mm square aluminium plate. Measurement uncertainty was assessed using a calibrated ballbar artefact traceable to an uncertainty of 2 µm with 38 mm diameter spheres and 500 mm separation between sphere centres. The plate and ballbar were positioned at a series of locations as shown in Figure 4.

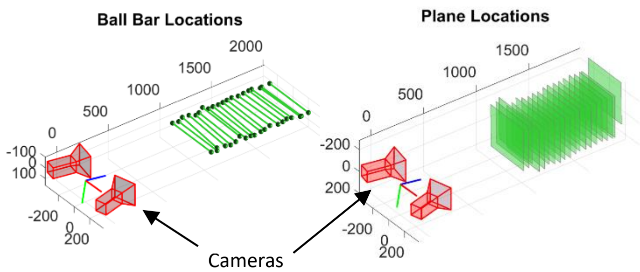

Figure 4. Scanner performance assessment artefact test locations, values given in mm.

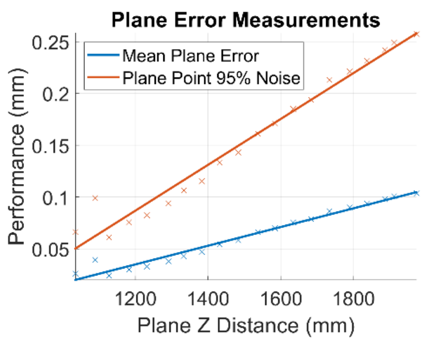

Figure 5. Scanner point noise as a function of distance from the scanner.

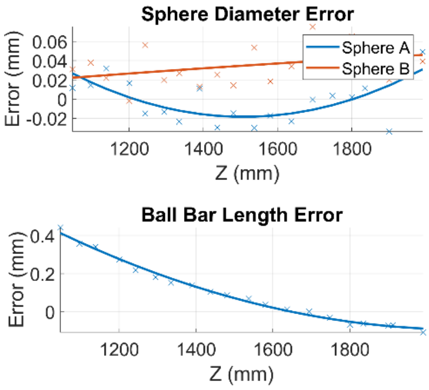

Figure 6. Scanner performance test results.

Scanner point noise is calculated using the distances from measured points to a least square fitted plane. The test results are shown in Figure 5, which plots the magnitude of the 95th percentile of point deviation from the fitted plane, and the mean deviation of points from the plane. Point noise remains below 0.25mm over a 1 m deep working volume. Noise can be seen to increase with distance from the scanner, as expected due reducing spatial resolution and lower illumination intensity at further distances from the scanner. The errors associated with geometric measurements of the ballbar can be seen in Figure 6. The 38 mm spheres were measured by least square sphere fitting to points measured on each sphere surface, giving a maximum error of 0.06 mm over the one metre deep working volume. The Ballbar length was estimated based on the two sphere centres, and this gave a standard deviation of 0.16 mm and mean error of 0.1 mm over the measurement depth, with a maximum error of 0.4 mm. The ballbar length error shows a systematic scaling error, with the error increasing as the measurement stand-off distance reduces. This reflects the calibration that was done using the HP Scan Pro v5 calibration artefact that was positioned a target location approximately 1.5 m from the scanner and indicates the potential to improve performance with an improved calibration.

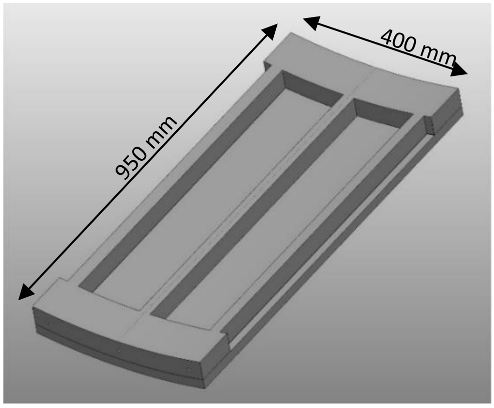

Figure 7. CAD model of concrete test part.

4. Net shape manufacturing

To evaluate the ability of the hybrid 3DCP system to produce complex geometry, a test part that includes curved surfaces and slender ribs that run the full length of the part is shown in Figure 7. The test part is similar, for example, to ribbed architectural cladding panels. In this example, the overall geometry would be important for aesthetic reasons, allowing multiple panels to tessellate, and the positions and size of the stiffening ribs would be important to ensure the structural performance of the part, and to allow alignment with fixing points; note these are hypothetical examples to illustrate the need for precision when manufacturing such a part. The CAD model of the test part is shown in Figure 7.

Figure 8. Photograph of the test part following the deposition stage, showing the poor overall geometry due to the material rheology, large nozzle size and high deposition rate.

The first stage of the hybrid process is to deposit concrete using the robot guided deposition nozzle. Robot tool paths were generated from the CAD model, using Autodesk PowerMill software [12]. To keep the process economical, high deposition rates are desirable, so a large 30 mm diameter nozzle was used, and the deposited layers were 13.5 mm thick. The robot was set to move the nozzle at a target speed of 50 mm/s. The high deposition rate, combined with the rheological properties of the wet concrete, that tends to sag and flow laterally during deposition, results in a deposited structure that is far from the target geometry, however the large concrete part can be deposited in approximately 18 minutes.

Figure 9. Milled concrete part, midway through the milling process, the edges and ends have received two passes, however the central rib has only been machined once.

For the second, milling stage, of the hybrid process, the wet concrete was left to cure partially so that it reaches a solidified, but not fully hardened state. This has the advantage of allowing easier material removal with significantly lower cutting forces as compared to machining fully hardened concrete. Milling tool paths were generated using Autodesk PowerMill software, and the robot was set to target a tool-tip traverse speed of 100 mm/s. The milling process, including pauses for manual removal of milled debris from the workpiece, took approximately 75 minutes. Compared to the time required to manufacture mould tooling, which can take days to weeks, this represents a significant speed increase. Figure 9 shows an image of the partially milled test part. It must be noted that the milling process is still in development, and work is required to improve the surface finishing with multiple finishing passes. Here, the ends of the part and the outer edges have received two milling passes; however, the central rib has only received one milling pass, hence the central rib is noticeably thicker.

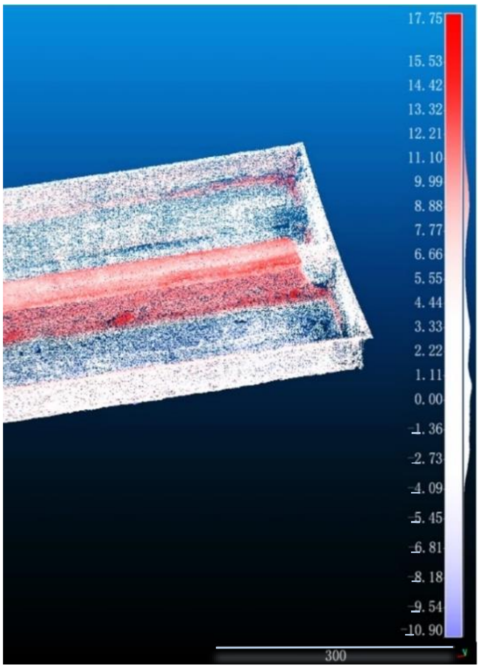

Figure 10. Colour coded point cloud, of the central section of the test part, illustrating deviation from CAD model, with all units in mm.

To measure the geometry of the milled part a method similar to that applied in [13] was followed. Geometric measurements were taken using the structured light scanner at a range viewpoints. The acquired point clouds were aligned and merged using an Iterative Closest Point (ICP) alignment algorithm within the opensource software CloudCompare. Then, the merged part point cloud was aligned and compared with the CAD model to attain the dimensional deviations from the target geometry. The results from the comparison to CAD are shown in Figure 10 and 11. In Figure 10 the central partially milled section has been segmented from the total point cloud showing that the milled edge sections have geometric deviations of approximately one millimetre, while the partially milled section of the central rib has a geometric deviation or approximately 10 mm. In Figure 11 the outer fully milled section of the point cloud has been segmented, and this shows that while many measured points are now within a few millimetres of the target geometry, there is evidence of some systematic error; for example, the upper faces being slightly higher than expected. This type of error may result from the robotic system calibration, and work is ongoing to investigate enhanced accuracy approaches based on detailed robot calibration, and closed loop control approaches.

5. Conclusions and future work

This work presented a hybrid 3DCP system with a custom built structured light scanner that can be used for process measurement and control. The performance of the scanner was assessed, and it was shown that the expected scanner measurement uncertainty is acceptable for the application of precision concrete manufacture, were parts of a few metres in size must be manufactured with tolerances of around one millimetre. The ability to manufacture complex concrete parts using 3DCP, with geometric precision of a few millimetres and potentially better was shown. Current work is now focusing on making use of the scanner as part of an adaptive milling approach to provide enhanced manufacturing accuracy.

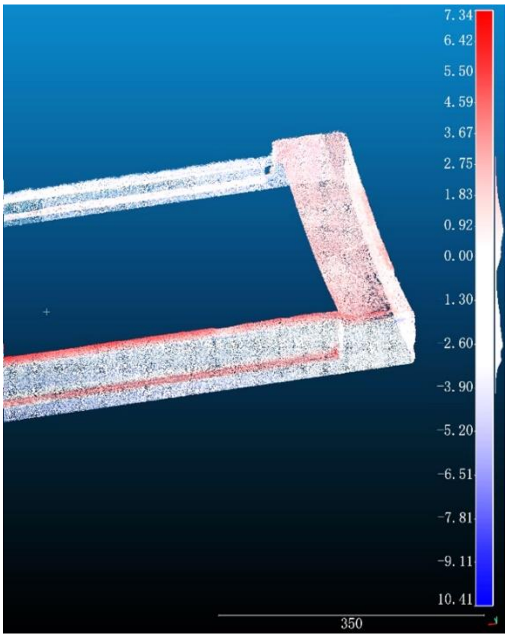

Figure 11. Colour coded point cloud, of outer fully milled section of the test part, illustrating deviation from CAD model, with all units in mm.

Acknowledgements

The authors wish to acknowledge support of the UK Engineering Physical Science and Research Council (EPSRC) for funding this work as part of grant numbers EP/S031405/1 and EP/L01498X/1.

References

[1] Lim S, Buswell R A, Le T T, Austin S A, Gibb A G, Thorpe T 2012 Developments in construction-scale additive manufacturing processes Automation in construction 21:262-8.

[2] Le TT, Austin SA, Lim S, Buswell RA, Law R, Gibb AG, Thorpe T 2012 Hardened properties of high-performance printing concrete. *Cement and Concrete Research* **42**(3):558-66.

[3] Le T T, Austin S A, Lim S, Buswell R A, Gibb A G, Thorpe T 2012 Mix design and fresh properties for high-performance printing concrete *Materials and structures* **45**(8), 1221-1232.

[4] Leach N, Carlson A, Khoshnevis B, Thangavelu M 2012 Robotic construction by contour crafting: The case of lunar construction. *International Journal of Architectural Computing*, **10**(3), 423-438.

[5] Bos F, Wolfs R, Ahmed Z, Salet T 2016 Additive manufacturing of concrete in construction: potentials and challenges of 3D concrete printing. *Virtual and Physical Prototyping*, **11**(3), 209-225.

[6] Buswell R A, De Silva W L, Jones S Z, Dirrenberger J 2018 3D printing using concrete extrusion: A roadmap for research *Cement and Concrete Research*, **112**, 37-49.

[7] Cobod International A/S, *Construction of Buildings on Demand* [online], accessed March 2021, https://cobod.com/

[8] Baumit GmbH, *Pioneer in concrete printing*, [online], accessed March 2021, https://baumit.at/bauminator

[9] Saint-Gobain, *Saint-Gobain Weber helps design 3D houses*, [online] April 2018, https://www.saint-gobain.com/en/saint-gobain-weber-helps-design-3d-houses.

[10] Milberg C T, Tommelein I D, 2020 Methods for managing tolerance compatibility: Windows in cast-in-place concrete *Journal of Construction Engineering and Management*, **146**(2), 04019105.

[11] Cavalaro, S. H. P., Blom, C. B. M., Aguado, A., & Walraven, J. C. (2012). New design method for the production tolerances of concrete tunnel segments. Journal of performance of constructed facilities, 26(6), 824-834.

[12] https://www.autodesk.co.uk/products/powermill/overview

[13] Xu J, Buswell R A, Kinnell P, Biro I, Hodgson J, Konstantinidis N, Ding L, 2020 Inspecting manufacturing precision of 3D printed concrete parts based on geometric dimensioning and tolerancing *Automation in Construction*, **117**, 103233.